M2AN - Modélisation mathématique et analyse numérique

Timo Tiihonen

Shape optimization and trial methods for free boundary problems

M2AN - Modélisation mathématique et analyse numérique, tome 31, nº 7 (1997), p. 805-825

<http://www.numdam.org/item?id=M2AN_1997__31_7_805_0>

MATHEMATICAL MODELLING AND NUMERICAL ANALYSIS
MODÉLISATION MATHÉMATIQUE ET ANALYSE NUMÉRIQUE

(Vol 31, n° 7, 1997, p 805 à 825)

SHAPE OPTIMIZATION AND TRIAL METHODS FOR FREE BOUNDARY PROBLEMS (*)

by Timo TIIHONEN [1]

Abstract — *In this work we consider different formulations for a free boundary problem and analyze the related numerical methods In particular, we formulate various shape optimization problems that are weak forms of a free boundary problem and analyze their properties using the tools of « shape calculus » The main result is that it is possible to influence the conditioning of the shape cost functional and to find a formulation which leads to optimally conditioned shape hessian at the solution We also analyze and compare some fixed point type methods inspired by the shape optimization problems*

Key words · free boundary problems, shape optimization, shape sensitivity analysis, fixed point methods.

1980 *Mathematics subject classifications* 35R35, 49Q10, 65P05

Résumé — *Dans ce travail nous considérons plusieurs formulations différentes d'un problème de frontière libre et analysons des méthodes numériques correspondantes En particulier, nous allons formuler plusieurs problèmes d'optimisation de forme qui sont des formulations faibles d'un problème de frontière libre Puis, nous analysons des propriétés des formulations différentes avec les outils du « calcul de forme » Le résultat principal est que c'est possible d'influencer le conditionnement de fonction à minimiser et trouver une formulation où l'Hessian par rapport à la forme soit optimal du point de vue de conditionnement. Nous étudions aussi des méthodes de type point fixé inspirées par les problèmes d'optimisation de forme*

1. INTRODUCTION

In this work we shall consider the famous Alt-Caffarelli problem [1]. That is, the problem of finding Σ, the free boundary, so that

$$\begin{cases} -\ \Delta u = 0 & \text{in } \Omega, \\ u = 1 & \text{on } \Gamma, \\ u = 0 & \text{on } \Sigma, \\ \dfrac{\partial u}{\partial n} = \lambda & \text{on } \Sigma \end{cases} \tag{1.1}$$

(*) Manuscript received January 2, 1996 Accepted July 17, 1996
[1] Department of Mathematics, University of Jyvaskyla, Box 35, FIN-40351 Jyvaskyla, Finland

for given $\lambda < 0$ and Γ, see *figure* 1.

It is well known [1], that the solution of (1.1) is a critical point of the following energy

$$E(\Omega, u) = \frac{1}{2}\int_{\Omega} \nabla u \, \nabla u + \frac{1}{2}\int_{\Omega} \lambda^2 \tag{1.2}$$

with respect to Ω and $u \in V(\Omega) = \{v \in H^1(\Omega) \mid v|_{\Gamma} = 1, v|_{\Sigma} = 0\}$. If λ is a negative constant and Γ is a Lipschitz curve then the solution exists and Σ is a C^{∞} curve (in 2-D case) [1].

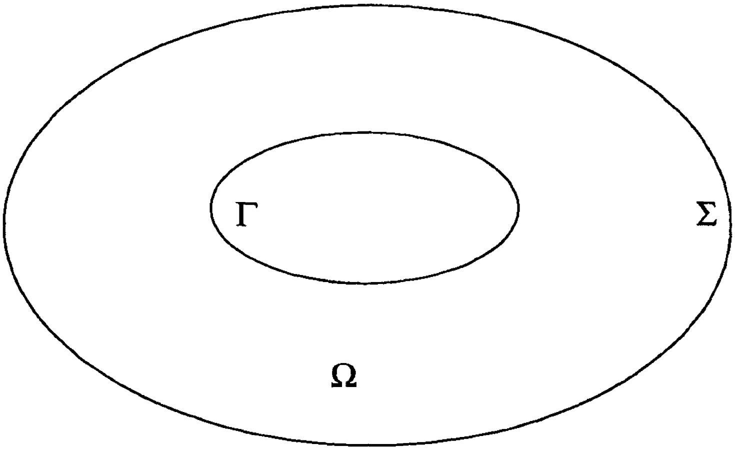

Figure 1. — Σ is free boundary, Γ is given.

Obviously, there are also other possibilities to formulate the free boundary problem as a minimization problem. For example, we can introduce the shape optimization problem :

$$\text{Minimize } J(\Omega) = \int_{\Sigma} u^2 \, d\Sigma \,, \tag{1.3}$$

where u solves the boundary value problem

$$\begin{cases} -\ \Delta u = 0 & \text{in } \Omega, \\ u = 1 & \text{on } \Gamma, \\ \dfrac{\partial u}{\partial n} = \lambda & \text{on } \Sigma . \end{cases} \tag{1.4}$$

If Σ is free boundary then $J(\Omega) = 0$. So any solution of the free boundary problem is also a solution of the minimization problem. In general (when the existence of a solution to the free boundary problem is not guaranteed *a priori*) we can not, however, deduce that a solution of the minimization problem (if it exists) would also solve the free boundary problem. In this sense this formulation is thus weaker than the Alt-Caffarelli formulation.

Now the following question can be raised ; which of the above two formulations leads in practice to more efficient numerical procedure. Or more generally, what is the « best » way to formulate the above problem as a shape optimization problem ? To give a partial answer to the above question we shall analyze the Hessians of the cost functionals. We shall also formulate some fixed point type methods and analyze their convergence with the tools provided by the shape calculus. Although our goal is to derive numerical methods the analysis is made on the level of continuous problems so that the conclusions should be valid independently of discretization methods. Hence, our main reference to shape optimization machinery is the book of Sokolowski and Zolésio [10]. However, in actual implementation of the methods described here some backgroud in numerical treatment of shape optimization problems is needed, see for example [8] and [9].

The structure of the paper is as follows. In the chapter 2 we recall the basic tools of shape calculus. Then we apply the tools to compute the shape Hessians of (1.2) and (1.3). We are then able to propose a formulation analogous to (1.3), (1.4) that is optimal from the point of view of the conditioning of the cost function. In chapter 5 we introduce and analyze some fixed point methods and discuss their connections to the shape optimization formulations. In chapter 6 we compare the convergence of different methods.

2. RECALL ON SHAPE CALCULUS

In this chapter we shall briefly recall some basic concepts and results related to shape differentiation [3], [4], [5], [13]. Assume that Ω is a smooth domain contained in a larger smooth domain D. Let us denote by V a vector field defined in D, $V \in C^k(D ; \mathbb{R}^n)$, $V|_{\partial D} = 0$. By T_t we denote the mapping $T_t x = x + tV(x)$, which for t small enough is smooth one to one mapping from D into itself. The image of Ω under T_t is denoted by Ω_t.

Let there now be defined a domain functional $J : \Omega \to \mathbb{R}$. We say that the functional has a *directional Eulerian shape derivative* to direction V at Ω if the limit

$$\lim_{t \to 0+} \frac{J(\Omega_t) - J(\Omega)}{t} =: DJ(\Omega ; V)$$

exists. If further $DJ(\Omega ; V)$ is linear and continuous with respect to V, we say that J is *shape differentiable* at Ω. The Hadamard structure theorem tells further that $DJ(\Omega ; V)$ depends only on the normal component of V on the boundary of Ω [12].

For function $y(t, x)$ defined in $[0, T] \times D$ we define the material derivative as a limit

$$\dot{y}(x) := \lim_{t \to 0} \frac{y(t, T_t x) - y(0, x)}{t}$$

and the shape derivative as

$$y'(x) := \lim_{t \to 0} \frac{y(t, x) - y(0, x)}{t} \quad (= \dot{y} - \nabla y \cdot V) .$$

y' can be defined uniquely in Ω also in the case when $y(t, x)$ is defined only for $x \in \Omega_t$.

We are now ready to formulate the basic formulas for shape differentiation of integrals : let $f \in L^1(\Omega)$ and assume that there exist $\dot{f} \in L^1(\Omega)$ and $f' \in L^1(\Omega)$. Then for Ω and V smooth enough

$$\frac{d}{dt} \int_{\Omega_t} f(t, x)\, dx \,|_{t=0} = \int_{\Omega} f'(0, x)\, dx + \int_{\partial\Omega} f(0, s) \langle V, n \rangle\, ds . \tag{2.1}$$

Similarly, if $f \in L^1(\Gamma)$ and there exist $\dot{f} \in L^1(\Gamma)$ and $f' \in L^1(\Omega)$, then

$$\frac{d}{dt} \int_{\Gamma_t} f(t, s)\, ds \,|_{t=0} = \int_{\Gamma} f'(0, s)\, ds + \int_{\Gamma} \left(\frac{\partial f}{\partial n} + fH \right) \langle V, n \rangle\, ds . \tag{2.2}$$

Here H is the mean curvature of Γ.

Let us now apply the above tools to calculate the shape derivative of

$$J(\Omega) = \int_{\Sigma} u^2\, d\Sigma \tag{2.3}$$

when u is the solution of the problem

$$\begin{cases} -\ \Delta u = 0 & \text{in } \Omega, \\ u = 1 & \text{on } \Gamma, \\ \alpha u + \dfrac{\partial u}{\partial n} = \lambda & \text{on } \Sigma . \end{cases} \tag{2.4}$$

That is, we consider a variant of (1.3), (1.4). Assume that $V = 0$ on Γ and $\alpha \geqslant 0$ is fixed. The shape derivative of J could be now determined directly by introducing *Lagrangian functional* [3], [5]

$$L(t, \varphi, \psi) = \int_{\Omega_t} \nabla\varphi\, \nabla\psi + \int_{\Sigma_t} (\alpha\varphi - \lambda)\, \psi + \varphi^2$$

and applying the results of Delfour-Zolesio [5]. For our purposes the approach that relies on the shape differentiability of the solution of (2.4) is, however, better adapted.

Let us first write (2.4) in variational form :

$$\int_{\Omega} \nabla u \nabla \varphi + \int_{\Sigma} \alpha u \varphi = \int_{\Sigma} \lambda \varphi \quad \varphi \in H^1(\Omega ; \Gamma), \tag{2.5}$$

$u \in H^1(\Omega)$, $u|_{\Gamma} = 1$. If Ω and the velocity field V are regular enough, then the solution u is shape differentiable and we can differentiate (2.5) to get

$$\begin{aligned}\int_{\Omega} \nabla u' \nabla \varphi + \int_{\Sigma} \alpha u' \varphi = \int_{\Sigma} \Big[&- \nabla u \nabla \varphi \langle V, n \rangle \\ &- \alpha\Big(\frac{\partial u}{\partial n} + uH\Big) \varphi \langle V, n \rangle + \lambda H \varphi \langle V, n \rangle \Big] .\end{aligned} \tag{2.6}$$

From this we can derive a boundary value problem for u'. Namely choosing $\varphi \in C_0^{\infty}(\Omega)$ and integrating by parts we get

$$-\int_{\Omega} \Delta u' \varphi = 0 \quad \forall \varphi \in C_0^{\infty}(\Omega) . \tag{2.7}$$

Hence $-\Delta u' = 0$ in Ω. Now, choose $\phi \in C^{\infty}(\Sigma)$. We can now find an extension $\varphi \in C^{\infty}(\Omega)$ such that $\varphi|_{\Sigma} = \phi$, $\frac{\partial \varphi}{\partial n}\Big|_{\Sigma} = 0$. Integrating by parts in (2.6) and using (2.7) we get

$$\int_{\Sigma} \Big(\frac{\partial u'}{\partial n} + \alpha u'\Big) \phi = \int_{\Sigma} - \nabla_{\Sigma} u \nabla_{\Sigma} \phi \langle V, n \rangle - \alpha\Big(\frac{\partial u}{\partial n} + uH\Big) \phi \langle V, n \rangle + \lambda H \phi \langle V, n \rangle ,$$

where $\nabla_{\Sigma} u = \nabla u - n \frac{\partial u}{\partial n}$ is the tangential component of the gradient.

We can integrate by parts on Σ to get

$$\frac{\partial u'}{\partial n} + \alpha u' = \nabla_{\Sigma} . (\langle V, n \rangle \nabla_{\Sigma} u) - \alpha\Big(\frac{\partial u}{\partial n} + uH\Big) \langle V, n \rangle + \lambda H \langle V, n \rangle .$$

Combining the above we conclude that the shape derivative u' is the solution of the problem

$$\begin{aligned}\int_{\Omega} \nabla u' \nabla \varphi + \int_{\Sigma} \alpha u' \varphi = \int_{\Sigma} &- \nabla_{\Sigma} u \nabla_{\Sigma} \varphi \langle V, n \rangle \\ &- \alpha\Big(\frac{\partial u}{\partial n} + uH\Big) \varphi \langle V, n \rangle + \lambda H \varphi \langle V, n \rangle .\end{aligned} \tag{2.8}$$

The shape derivative of J can now be expressed as

$$DJ(\Omega\,;V)=\int_{\Omega} 2\,uu'+\int_{\Sigma} u^2\,\langle V,n\rangle\,.$$

Other cost functionals can be treated in analogous way. The case when the state problem has Dirichlet boundary condition on the optimized boundary results to a Dirichlet problem for the shape derivative u'. The boundary condition for u' reads in this case [12]

$$u'=-\frac{\partial u}{\partial n}\langle V,n\rangle \text{ on } \Sigma\,.$$

To complete this brief recall, let us finally introduce the second order shape derivative of a shape functional. Assume that there are two smooth vector fields V and W defined in $[0,T]\times D$. Denote $\Omega_t(W)=T_t(W)(\Omega)$ with $T_t(W)$ being the transformation related to field W. Assume that $DJ(\Omega_t(W)\,;V(t))$ exists for all $t\in[0,T]$. The second order Eulerian semiderivative at Ω in directions V, W is defined as [3]

$$D^2\,J(\Omega\,;V,W)=\lim_{t\to 0}\frac{DJ(\Omega_t(W)\,;V(t))-DJ(\Omega\,;V(0))}{t}$$

whenever the limit exists.

Under suitable assumptions $D^2\,J(\Omega\,;V\,;W)$ has a decomposition

$$D^2\,J(\Omega\,;V,W)=D^2\,J(\Omega\,;V(0),W(0))+DJ(\Omega\,;\dot V(0))$$

with

$$\dot V(0)\,(x)=\lim_{t\to 0}\frac{V(t,x)-V(0,x)}{t}\,.$$

The second term vanishes if the field V is autonomous. The functional J is said to be twice shape differentiable at Ω if $D^2\,J(\Omega\,;V,W)$ exists and the map V, $W\to D^2\,J(\Omega\,;V,W)$ is bilinear and continuous for V, W in $\mathscr{D}(D,\mathbb{R}^n)$, ($\mathscr{D}$ is the space of test functions). The distribution associated with the above mapping is called the Shape Hessian. It can be shown that the Shape Hessian has its support at the boundary of Ω and it is independent on the tangential component of W on the boundary. On the other hand, the tangential component of V contributes to Shape Hessian in general. Hence the Shape Hessian is not symmetric in general. At critical point of J one can, however, prove that the Shape Hessian depends only on the normal components of V and W [13].

3. SHAPE VARIATIONAL PRINCIPLE

As already mentioned in the introduction the free boundary problem is equivalent to the minimization of the energy E of (1.2). This provides to us a conceptionally simple and appealing formulation of the free boundary problem which has turned out to be very efficient from the theoretical point of view. Also the optimality condition (3.1) below is simple and directly related to the free boundary condition.

However from the above properties we can not conclude if the resulting optimization problem is easy to solve or not. That is, how well do the standard minimization algorithms perform on this particular problem. This depends essentially on two points, how quadratic the energy is (far from the solution) and how well conditioned the quadratic part is (near the solution).

Let us now analyze the behavior of the energy near the solution. For that purpose we compute the second shape derivatives at the solution, the so called *Shape Hessian.*

Let V and W be two independent autonomous velocity fields. Then the derivative of $E(\Omega)$ to the direction V is

$$DE(\Omega ; V) = \int_\Omega \nabla u \, \nabla u'_V + \frac{1}{2}\int_\Sigma \nabla u \, \nabla u \, \langle V, n\rangle + \frac{1}{2}\int_\Sigma \lambda^2 \langle V, n\rangle$$

where u'_V is the shape derivative of u into direction V. Now integrating by parts we obtain

$$\int_\Omega \nabla u \, \nabla u'_V = \int_\Sigma \frac{\partial u}{\partial n} u'_V$$

as $\Delta u = 0$ in Ω. As u is the solution of a Dirichlet problem we know that $u'_V = -\frac{\partial u}{\partial n}\langle V, n\rangle$ on Σ. Moreover $\nabla u \, \nabla u = \left(\frac{\partial u}{\partial n}\right)^2$ on Σ. Hence we have for $DE(\Omega ; V)$ the expression

$$DE(\Omega ; V) = -\frac{1}{2}\int_\Sigma |\nabla u|^2 \langle V, n\rangle + \frac{1}{2}\int_\Sigma \lambda^2 \langle V, n\rangle . \tag{3.1}$$

Thus any solution of the free boundary problem is a critical point of E as $\frac{\partial u}{\partial n} = \lambda$ and $u = 0$ imply that $|\nabla u|^2 = \lambda^2$.

By applying the Stokes theorem, we get further

$$DE(\Omega ; V) = \frac{1}{2}\int_\Omega \operatorname{div}\left(V(\lambda^2 - |\nabla u|^2)\right) .$$

For the second order derivative we have first

$$D^2 E(\Omega ; V, W) = -\int_\Omega \operatorname{div}(V \nabla \dot{u} \nabla u'_W)$$

$$+ \frac{1}{2}\int_\Sigma \operatorname{div}(V(\lambda^2 - |\nabla u|^2))\langle W, n\rangle = I_1 + I_2 .$$

Applying once more the Stokes theorem we get at the solution of the free boundary problem

$$I_1 = -\int_\Sigma \nabla u'_W \nabla u \langle V, n\rangle = -\int_\Sigma \frac{\partial}{\partial n} u'_W \lambda \langle V, n\rangle .$$

Now, if we denote by S the *Steklov-Poincare* operator on Σ, i.e. the Dirichlet to Neumann map which is defined by

$$S\mu = \left.\frac{\partial v}{\partial n}\right|_\Sigma \tag{3.2}$$

for v being solution of

$$\begin{cases} -\ \Delta v = 0 & \text{in } \Omega \\ v = 0 & \text{on } \Gamma \\ v = \mu & \text{on } \Sigma . \end{cases}$$

Then we can write at the solution

$$\frac{\partial u'_V}{\partial n} = S u'_V = -S\lambda \langle V, n\rangle . \tag{3.3}$$

Thus

$$I_1 = (\langle V, n\rangle \lambda, S\lambda \langle W, n\rangle) .$$

The second term can be written as

$$I_2 = \frac{1}{2}\int_\Sigma \operatorname{div} V(\lambda^2 - |\nabla u|^2)\langle W, n\rangle$$

$$+ \frac{1}{2}\int_\Sigma V_\Sigma . \nabla_\Sigma(\lambda^2 - |\nabla u|^2)\langle W, n\rangle$$

$$+ \frac{1}{2}\int_\Sigma \langle V, n\rangle \frac{\partial}{\partial n}(\lambda^2 - |\nabla u|^2)\langle W, n\rangle .$$

At the solution of the free boundary problem we have $\lambda^2 = |\nabla u|^2$. Hence the first two terms disappear. The last term can be written as

$$- \int_{\Sigma} \langle V, n \rangle \langle W, n \rangle \frac{\partial u}{\partial n} \frac{\partial^2 u}{\partial n^2} .$$

If we now exploit the well known decomposition of Δu [10], [12],

$$\Delta u = \varDelta_{\Sigma} u + H \frac{\partial u}{\partial n} + \frac{\partial^2 u}{\partial n^2} ,$$

where $\varDelta_{\Sigma}$ is the *Laplace-Beltrami* operator on Σ and recall that $\varDelta_{\Sigma} u = 0$ on the boundary, we get

$$\frac{\partial^2 u}{\partial n^2} = - H \frac{\partial u}{\partial n} .$$

Hence

$$I_2 = \int_{\Sigma} \langle V, n \rangle \langle W, n \rangle \left(\frac{\partial u}{\partial n} \right)^2 H$$

and we get the final expression for the shape Hessian :

PROPOSITION 1 : *At any critical point of the energy E the shape Hessian of E has the expression*

$$D^2 E(\Omega ; V, W) = (\langle V, n \rangle \lambda, (S + IH) \langle W, n \rangle \lambda) . \tag{3.4}$$

As the operator S maps the Sobolev space $H^l(\Sigma)$ into $H^{l-1}(\Sigma)$, the minimal regularity for (3.4) to make sense is that V and W belong to $H^{1/2}(\Sigma)$. This means, among other things that in the discrete case the condition number of the Hessian of the cost function increases when the discretization of the free boundary is refined unless the basis of $H^{1/2}(\Sigma)$ is used for characterization of the discrete geometries.

4. GENERAL SHAPE OPTIMIZATION FORMULATION

Let us now analyze the strategy of presenting the free boundary problem as a shape optimization problem where the cost function is obtained from one of the free boundary conditions. In particular we shall consider the problem : Find Ω (or Σ) so that the cost

$$J(\Omega) = \frac{1}{2} \int_{\Sigma} u^2 \tag{4.1}$$

is minimized, where u is the solution boundary value problem

$$\begin{cases} -\ \Delta u = 0 & \text{in } \Omega \\ u = 1 & \text{on } \Gamma \\ \alpha u + \dfrac{\partial u}{\partial n} = \lambda & \text{on } \Sigma . \end{cases} \tag{4.2}$$

Here $\alpha \geqslant 0$ can be chosen freely as in any case at the solution of the free boundary we have $\alpha u = 0$.

A natural question is how to choose α so that the minimization problem is easy to solve. It turns out that $\alpha = H$, the mean curvature of Σ, is a good choice as we have

LEMMA 1 : *Let $\alpha = H$ in (4.2). Then if Σ is the free boundary, the shape derivative u' of the solution of (4.2) vahishes.*

Proof: Applying the formula (2.8) at the solution of the free boundary problem (when $u = 0$ on Σ) we obtain that the shape derivative u' satisfies the equation

$$\int_{\Omega} \nabla u' \nabla \varphi + \int_{\Sigma} \alpha u' \varphi = - \int_{\Sigma} \alpha \frac{\partial u}{\partial n} \varphi \langle V, n \rangle + \int_{\Sigma} \lambda H \varphi \langle V, n \rangle \quad \forall \varphi \in H^1(\Omega ; \Gamma) .$$

As $\dfrac{\partial u}{\partial n} = \lambda$, after choosing $\alpha = H$ the right hand side vanishes and $u' \equiv 0$.

Let us now analyze the shape Hessian of the optimal shape design problem. As in the previous chapter let V and W be two velocity fields. Then we easily obtain that the derivative of $J(\Omega)$ into direction V is

$$DJ(\Omega ; V) = \int_{\Sigma} u u'_V + \int_{\Sigma} u \frac{\partial u}{\partial n} \langle V, n \rangle + \frac{1}{2} \int_{\Sigma} u^2 H \langle V, n \rangle = I_1 + I_2 + I_3. \tag{4.3}$$

What about the second derivatives at the solution Ω where $u = 0$ on Σ. Easily we see that

$$DI_3(\Omega ; W) = 0 .$$

For I_2 we have

$$DI_2(\Omega ; W) = \int_{\Sigma} \left(u'_W + \frac{\partial u}{\partial n} \right) \langle W, n \rangle \frac{\partial u}{\partial n} \langle V, n \rangle .$$

Finally, for I_1 we get

$$DI_1(\Omega\,;W)=\int_{\Sigma}\left(u'_W+\frac{\partial u}{\partial n}\langle W,n\rangle\right)u'_W\,.$$

Hence

$$D^2 J(\Omega\,;V,W)=\int_{\Sigma}\lambda^2\langle W,n\rangle\langle V,n\rangle+\int_{\Sigma}u'_Wu'_V$$
$$+\int_{\Sigma}\lambda(u'_V\langle W,n\rangle+u'_W\langle V,n\rangle)\,. \tag{4.4}$$

So in the case $\alpha=H$ we have that $u'_V=u'_W=0$ and, consequently, we obtain

PROPOSITION 2 : *If (u,Σ) is a solution of the free boundary problem, then the shape Hessian of the energy (4.1) is equal to*

$$D^2 J(\Omega\,;V,W)=\int_{\Sigma}\lambda^2\langle W,n\rangle\langle V,n\rangle\,.$$

when we choose $\alpha=H$ in (4.2).

Thus the Shape Hessian at the solution is essentially an identity operator. This means, among other things, that in the discrete case the condition number of the Hessian matrix can be made independent of the mesh size. Moreover, an optimal preconditioner can be constructed from the « mass » matrix corresponding to the basis chosen for the deformation velocities.

Let us also analyze the case $\alpha=0$. Then at the solution of the free boundary problem the shape derivatives satisfy the problem

$$\int_{\Omega}\nabla u'\,\nabla\varphi=\int_{\Sigma}\lambda H\varphi\,\langle V,n\rangle\,.$$

Integrating by parts we get

$$\frac{\partial u'}{\partial n_V}=H\langle V,n\rangle\,.$$

Thus, using the Steklov-Poincare operator defined in (3.2) we can write

$$Su'_V=\lambda H\langle V,n\rangle$$

or

$$u'_V = S^{-1}(\lambda H \langle V, n \rangle) .$$

Combining this with (4.4) we arrive to

PROPOSITION 3 : *When we choose* $\alpha = 0$ *in (4.2) the shape Hessian at the solution of the minimization problem reads*

$$D^2 J(\Omega ; V, W) = \int_\Sigma (S^{-1}(\lambda H \langle V, n \rangle) + \lambda \langle V, n \rangle) \times (S^{-1}(\lambda H \langle W, n \rangle) + \lambda \langle W, n \rangle) . \quad (4.5)$$

As S^{-1} is a bounded operator the Shape Hessian is well conditioned also in this case. An optimal preconditioner may, however, be harder to obtain than in the case $\alpha = H$.

Making comparison to the shape variational principle we notice that in our example the general shape optimization formulation results to problems that are better conditioned than the variational principle. The prize to pay is the more involved the computation of the gradient during the minimization. This means that in practice the adjoint system has to be solved on every iteration. In shape variational principle no adjoint state is needed.

5. FIXED POINT METHODS

From the practical point of view the formulation of free boundary problems as shape optimization problem necessitates some tools. The most important point is the requirement of a reliable optimization algorithm. There are several good algorithms available in various solftware libraries. However, to combine them with given PDE solver is not a trivial thing. First of all, the PDE solver has to be sub-ordinated to the optimization routine. This can be technically difficult, especially when working with commercial solvers. Secondly, the good optimization algorithms rely on the use of gradient information. Thus their use requires some sensitivity analysis. In many cases it would be useful to have a method that solves the free boundary using some simple updating formula based on the solution of some state problem.

We shall now consider the previously mentioned shape optimization problems from the point of view of deriving fixed point type rules.

The shape variational principle provides us a first candidate for a fixed point algorithm as it leads to minimization problem with gradient depending on the solution of the state problem alone. Thus applying steepest descent method with constant step size will give an explicit fixed point type algorithm. The free boundary Σ is to be moved to the direction of the negative gradient

$$\frac{1}{2}\left[\left(\frac{\partial u}{\partial n}\right)^2 - \lambda^2\right]$$

which can be easily evaluated once the state problem is solved. However, the iteration will not converge in the continuous case. This is because the Hessian of the problem is unbounded and the steepest descent method will diverge with any constant step length. In the discrete case the step length (and hence the convergence rate) has to be decreased as a function of grid refinement.

A possible remedy is to apply preconditioning, that is, to change the norm in the space of design variables. According to Proposition 1 the leading term in the Shape Hessian is the Steklov-Poincare operator. Hence, if we change the inner product of the design space to the inner product of $H^{1/2}(\Sigma)$ the Shape Hessian becomes bounded. In practice this can be done by multiplying the search direction with S^{-1}. S^{-1} can be considered as an approximation for the inverse of the Shape Hessian. Of course, we can also take into account the lower order terms in the Shape Hessian which leads to multiplying the search direction by $(S + I\alpha)^{-1}$ where α is an estimate for the mean curvature H of the free boundary.

The scheme can be formulated as

Algorithm 1 (Inexact Newton)

(1) Choose Σ^0, $\alpha \geqslant 0$ (approximation to the mean curvature of the solution). Set $n = 0$.

(2) Solve the Dirichlet problem in Ω^n.

(3) Solve the auxiliary problem $y = \lambda^{-2}(S + \alpha I)^{-1}\nabla E$. That is,

$$-\Delta y = 0\,, \quad \text{in } \Omega\,,$$

$$y = 0 \quad \text{on } \Gamma\,,$$

$$\alpha y + \frac{\partial y}{\partial n} = \frac{1}{2}\left[\left(\frac{\partial u}{\partial n}\right)^2 - \lambda^2\right]/\lambda^2 \quad \text{on } \Sigma\,. \tag{5.1}$$

(4) Set $\Sigma^{n+1} = \Sigma^n + \mathcal{N}y$, where $\mathcal{N}$ is a regularization of the unit normal to Σ^n.

(5) If y is small enough, then stop. Otherwise, set $n = n + 1$ and continue from 2.

For shape optimization formulations the use of steepest descent would require the evaluation of the gradient of the cost function using the adjoint state technique for example. Using lemma 1, a closer look at the gradient (4.3) reveals, however, that if we choose $\alpha \approx H$ in the state problem (3.2) and restrict our attention to the neighborhood of the solution, the leading term is

$$\int_{\Sigma} u \frac{\partial u}{\partial n} \langle V, n \rangle .$$

As at the solution $\frac{\partial u}{\partial n} = \lambda$ and Shape Hessian is λ^2 times the identity, the steepest descent method with optimal step length approaches the rule

$$\Sigma^{n+1} = \Sigma^n - \frac{u}{\lambda} \mathcal{N} . \tag{5.2}$$

This leads to a method known already by Garabedian [7], see also Cuvelier-Schulkes [2], Tiihonen-Järvinen [11]. Additional regularization of the normal has to be made as otherwise the regularity of Σ would decrease on every iteration. This has been studied by Flucher and Rumpf [6] who have proved the superlinear convergence of the regularized fixed point iteration in the continuous case. In the discrete case implicit regularization is introduced by rules that define the discrete normal directions for polygonal domains.

Algorithm 2

(1) Choose Σ^0, $\alpha \geqslant 0$ as in Algorithm 1. Set $n = 0$.
(2) *Solve the Newton boundary value problem (4.2) in Ω^n.*
(3) Set $\Sigma^{n+1} = \Sigma^n - \mathcal{N} \frac{u}{\lambda}$.
(4) If $u|_{\Sigma}$ is small enough, then stop. Otherwise, set $n = n + 1$ and continue from 2.

In the derivation of the above algorithm it was assumed that $\alpha \approx H$. If this is not the case then the step 3 above is not optimal. For example in the case $\alpha = 0$ the leading part of the directional shape derivative is

$$\int_{\Sigma} u u'_V + \int_{\Sigma} u \frac{\partial u}{\partial n} \langle V, n \rangle = \int_{\Sigma} u (I + S^{-1} H) (\lambda \langle V, n \rangle)$$

at the solution. Taking this and expression (4.5) for the Shape Hessian into account we notice that the iteration (5.2) is close to steepest descent if $S^{-1} H$ is « small ». That is, if the free boundary is flat and the distance between Γ and Σ is small. In other cases additional damping has to be introduced, ideally by making the boundary correction with scheme

$$\Sigma^{n+1} = \Sigma^n - \mathcal{N} (I + S^{-1} H)^{-1} \frac{u}{\lambda} . \tag{5.3}$$

6. EXAMPLES

1. Axisymmetric case

Let us first consider a simple axisymmetric case. The main emphasis is of course on the fixed point method as the comparison of different one dimensional minimization problems does not make very much sense.

So we consider the free boundary problem

$$\begin{cases} -u_{rr} - \frac{1}{r} u_r = 0 \\ u(1) = 1\,, \\ u(S) = 0\,, \\ \frac{\partial u(S)}{\partial n} = -\lambda\,. \end{cases} \tag{6.1}$$

This problem has a unique solution $S_\lambda > 1$ for any $\lambda < 0$. Namely, the general solution has the form

$$u(r) = C_0 + C_1 \ln r\,.$$

Imposing the Dirichlet boundary conditions we can fix the coefficients to obtain

$$u(r) = 1 - \frac{\ln r}{\ln S}\,.$$

Then

$$\frac{\partial u(S)}{\partial r} = -\frac{1}{S \ln S}$$

is a monotonically increasing function of S attaining all negative values. The problem is therefore well posed. The Alt-Caffarelli energy E reads

$$E(S) = \frac{1}{2}\int_1^S \left[\left(\frac{1}{r \ln S}\right)^2 + \lambda^2\right] r\,dr = \frac{1}{2}\left[\frac{1}{\ln S} + \frac{\lambda^2(S^2-1)}{2}\right].$$

It has a unique minimizer which is the solution of our free boundary problem. Let us now consider the fixed point method (5.2). First, let us choose $\alpha = 0$ in the state problem, i.e. pure Neumann condition. Then $u(s) = 1 + \lambda S \ln S$ and (5.2) reads

$$S^{n+1} = F(S^n) = S^n - S^n \ln S^n - \frac{1}{\lambda}\,.$$

As $\frac{\partial F}{\partial S} = -\ln S$, the iteration converges locally if and only if $|\ln S| < 1$. This means that λ has to be smaller than $-\frac{1}{e}$ (compare with discussion at the end of chapter 5). The effect of the value of λ on the rate of convergence is illustrated in *figures* 2 and 3.

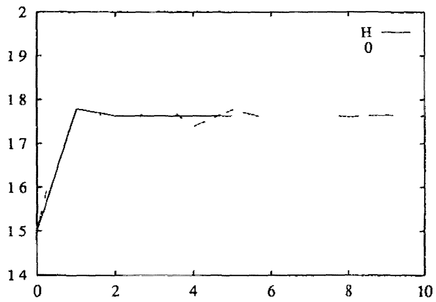

Figure 2. — λ = 1 0

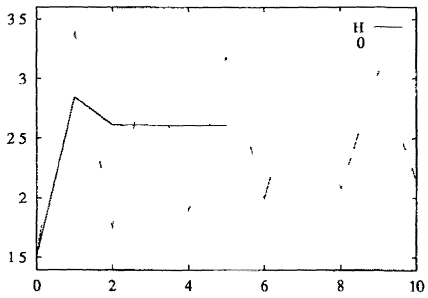

Figure 3. — λ = – 0 4

Let us now consider the Newton condition $Hu + \frac{\partial u}{\partial n} = \lambda$ in the state problem. The mean curvature H is $\frac{1}{S}$ in this case. Hence

$$u(S) = S\lambda - \frac{S\lambda - 1}{\ln S + 1}$$

and (5.2) reads

$$S^{n+1} = F(S^n) = S - S + \frac{S\lambda - 1}{(\ln S + 1)\,\lambda}$$

$$= \frac{S - \frac{1}{\lambda}}{(\ln S + 1)}.$$

Now

$$\frac{\partial F}{\partial S} = \frac{\ln S + 1 - \left(1 - \frac{1}{S\lambda}\right)}{(\ln S + 1)^2}.$$

As at the solution $\lambda = -\frac{1}{S \ln S}$, we have that, at the solution

$$\frac{\partial F}{\partial S} = 0$$

which implies superlinear (quadratic) convergence.

Some numerical experiments of using the fixed point method for the problem (6.1) are illustrated in *figures* 2 and 3. There we show the evolution of the free boundary as a function of iteration count for two different values of λ. Both Neumann and Newton conditions were used in the state problem. The initial guess for the free boundary was $S = 1.5$ in all cases.

2. Two dimensional examples

Let us now compare the different shape optimization formulations of the two dimensional free boundary problem. First we take a look at the formulation (4.1), (4.2) of the problem and study the role of the free parameter α. As indicated in chapter 4 a particularly interesting value for α is the mean curvature at the solution. As the solution is unknown we can not fix α to its optimal value beforehand. So two possibilities arise. Either we can use some rough estimate for α or we can try to deduce α from the mean curvature of the current approximation of the free boundary. It turns out that the latter alternative is not very robust. Any minor oscillation in Σ is amplified when the curvature is evaluated and often this results in oscillating boundary values for the solution of the state problem. Gradually, the oscillations are amplified and the overall convergence slows down or is lost completely, depending on the robustness of the outer iteration. For that reason, only the results from the first alternative are presented here.

In the numerical examples the problems were chosen so that the solution was axially symmetric. That is, we consider annular domains where the inner (fixed) boundary is circular. The initial approximation for the outer (free) boundary was chosen non-circular deliberately. By assuming sufficient symmetry from the data the computational domain was reduced to 1/8 :th of the annulus. This was discretized using 9×9 and 17×17 quadrilateral finite element grids. The radial coordinates of the nodal points of the outer surface were chosen as primal unknowns in optimization.

For optimization we used the algorithm E04UCF of the NAG subroutine library. The algorithm is an implementation of a Quasi-Newton method that uses sequential quadratic programming to determine the search directions. The method is generally efficient and robust. However, if the initial estimate for the Hessian is too inaccurate the first search directions can be far too long. This can be seen clearly in the numerical experiments where we have monitored both the function values and the norms of the gradients at every step where gradient is evaluated. Non-monotone behavior in the cost function history indicates that the algorithm has to make a line search in order to make a descending step.

In our numerical examples we chose the radius of the inner surface to be equal to one. The parameter λ was also one, leading to the final radius 1.76... for the outer surface. The gradients of cost functionals were evaluated using second order accurate finite differences with step length 10^{-5}. The initial guess for the geometry, together with the final solution is presented in *figure* 4.

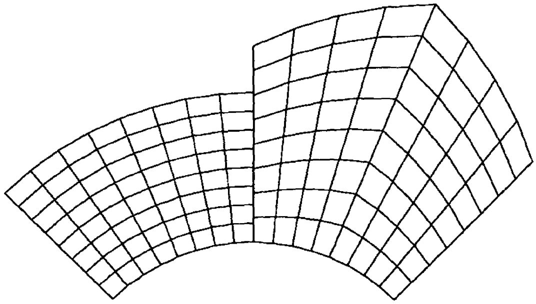

Figure 4. — Initial and final grids.

In *figures* 5 and 6 we show the evolution of the cost functional (4.1) against the number of gradient evaluations during the optimization. Two different cases, $\alpha = 0$ (lines B and b in the figures) and $\alpha = 1/2$ (A and a), were considered for two different grids. For each problem two different scalings of the cost function were used. With capital letters we denote the cases where there was no scaling. The lower case labeling refers to multiplication of the cost by $1/h$ which scales the effect of a single design variable to be of the same order of magnitude independently of the grid. Note that neither the function values nor the gradients are directly comparable for different scalings.

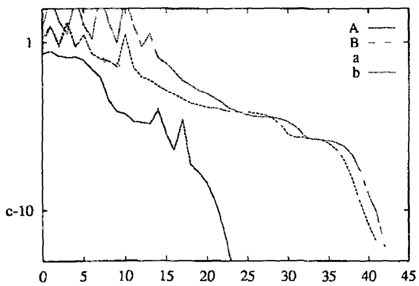

Figure 5. — Optimization history for 9×9 grid.

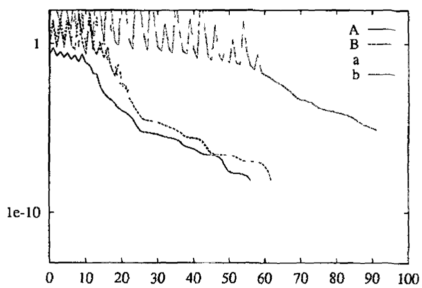

Figure 6. — Optimization history for 17×17 grid.

Clearly, the cases with $\alpha = 1/2$ lead to faster convergence. Let us remark that the value $\alpha = 1/2$ is a lower estimate for the curvature of the final solution. That particular value was chosen because it corresponds to the curvature of a circle with radius $1 + 1/\lambda$, which is the prediction of the free boundary when we assume linear radial profile for the solution.

To be able to compare the formulation (4.1), (4.2) with the shape variational principle we also tracked down the evolution in the norm of the gradient for each method. These are shown in *figures* 7 and 8. The shape variational principle (D and d, with same convention as above) seems to lead to faster

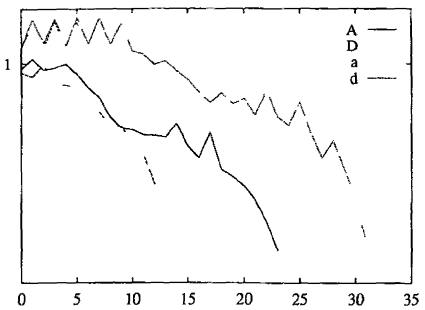

Figure 7. — Decay of gradient for 9 × 9 grid.

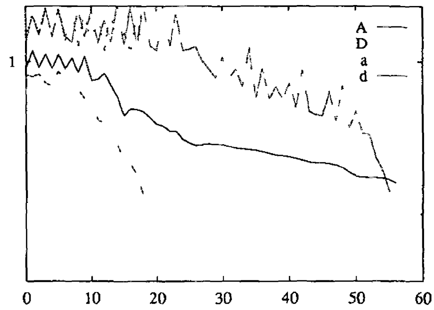

Figure 8. — Decay of gradient for 17 × 17 grid.

convergence in the case where the cost function is not scaled explicitly. In the case when we scale the cost (to effectively scale the initial Hessian matrix to be of order h for the original cost function) the situation is reversed. This scaling should be close to ideal for the formulation (4.1), (4.2). However, the overall performance of the scaled version is clearly inferior to the unscaled version for both algorithms. This seems to indicate that far from the solution the cost function is more strongly curved than near the optimum. Hence the algorithm tends to overshoot which makes the convergence slow. Also the second order information collected by the Quasi-Newton algorithm far from the solution is finally not useful near the optimum. Thus the superlinear convergence rate is obtained only after many iterations near the solution.

Next we compared the fixed point iterations presented in Chapter 5. The Algorithm 2 was tested with the same two values of α that were used for the optimization case (curves A $(\alpha = 1/2)$ and B $(\alpha = 0)$). The decay in the error of the free boundary condition $u = 0$ is shown in *figures* 9 and 10. The initial shape was the same as in the optimization case. For $\alpha = 0$ we also considered the damped iteration motivated by (5.3) (curve C) where the correction to Σ is multiplied by $(1 + \ln R)^{-1}$, where $R = 2$ is an estimate

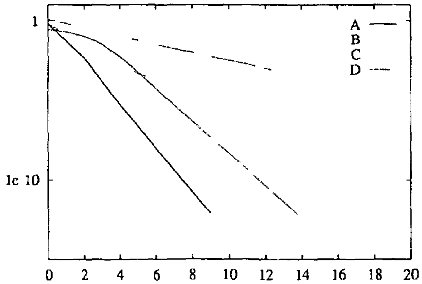

Figure 9. — Fixed point methods for 9 × 9 grid.

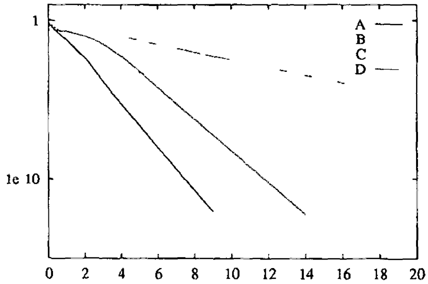

Figure 10. — Fixed point methods for 17 × 17 grid.

for the radius of the free boundary and $\ln R$ is an estimate for the norm of $S^{-1} H$. Finally by D we denote the iteration history corresponding to Algorithm 1, where the value of α was chosen to be 1/2.

To summarize the results of the numerical experiments we can observe that well preconditioned fixed point algorithms tend to converge at least as fast as the corresponding optimization algorithms. They are, however, easier to implement and do not require any numerical sensitivity analysis. Thus when solving stationary free boundary problems it seems advisable to analyze the problem and the potential fixed point rules by using the tools of shape calculus to obtain the optimal preconditioners.

REFERENCES

[1] H. W. ALT, L. A. CAFARELLI, 1981, *Existence and regularity for a minimum problem with free boundary,* J. Reine angew. Math **325,** 105-144.

[2] C. CUVELIER, R. M. S. M. SCHULKES, 1990, *Some numerical methods for the computation of capillary free boundaries governed by the Navier-Stokes equations,* Siam Review **32,** 355-423.

[3] M. C. DELFOUR, 1990, *Shape Derivatives and Differentiability of Min Max,* in « Shape Optimization and Free Boundaries, M. C. Delfour and G. Sabidussi (eds.) », Kluwer, Dordrecht, pp. 35-111.

[4] M. C. DELFOUR, J. P. ZOLÉSIO, 1991, *Anatomy of the shape Hessian,* Ann. Mat. Pura Appl. (4) **158,** 315-339.

[5] M. C. DELFOUR, J. P. ZOLÉSIO, 1991, *Velocity method and Lagrangian formulation for the computation of the shape Hessian,* SIAM J. Control Optim. **29,** 1414-1442.

[6] M. FLUCHER, M. RUMPF, 1997, *Bernoulli's free-boundary problem, qualitative theory and numerical approximation,* J. Reine angew. Math. **86.**

[7] P. R. GARABEDIAN, 1956, *The mathematical theory of three dimensional cavities and jets,* Bull. Amer. Math. Soc., **62,** 219-235.

[8] J. HASLINGER, P. NEITTAANMÄKI, 1996, « Finite element approximation for optimal shape, material and topology design », John Wiley.

[9] O. PIRONNEAU, 1984, « Optimal shape design for elliptic systems », Springer Verlag.

[10] J. SOKOLOWSKI, J. P. ZOLÉSIO, 1992, « Introduction to Shape Optimization », Springer Verlag.

[11] T. TIIHONEN, J. JÄRVINEN, 1992, *On fixed point (trial) methods for free boundary problems,* in « Free boundary problems in continuum mechanics », S. N. Antontsev, K.-H. Hoffmann, A. M. Khludnev (eds.), ISNM 106, Birkhäuser Verlag, Basel, pp. 339-350.

[12] J. P. ZOLÉSIO, 1979, « Identification de domaines par déformations », Thèse d'état, Univ. Nice.

[13] J. P. ZOLÉSIO, 1990, *Introduction to shape optimization problems and free boundary problems,* in « Shape Optimization and Free Boundaries », M. C. Delfour and G. Sabidussi (eds.), Kluwer, Dordrecht, pp. 397-457.

[14] J. P. ZOLÉSIO, 1994, *Weak Shape Formulation of Free Boundary Problems,* Ann. Scuola Norm. Sup. Pisa Cl. Sci., **XXI, 1,** 397-457.